THE JOURNAL OF BIOLOGICAL CHEMISTRY VOL. 288, NO. 5, pp. 3535–3544, February 1, 2013

Impaired Monoamine and Organic Cation Uptake in Choroid Plexus in Mice with Targeted Disruption of the Plasma Membrane Monoamine Transporter (*Slc29a4*) Gene*

Received for publication, November 15, 2012, and in revised form, December 11, 2012 Published, JBC Papers in Press, December 19, 2012, DOI 10.1074/jbc.M112.436972

Haichuan Duan and Joanne Wang[1]

From the Department of Pharmaceutics, University of Washington, Seattle, Washington 98195

Background: Some CNS active compounds are transported into or out of the brain by transporters in the choroid plexus (CP).
Results: PMAT is a major CP transporter for bioactive amines and xenobiotic cations.
Conclusion: PMAT transports organic cations from the cerebrospinal fluid into the CP.
Significance: PMAT may be an important determinant of brain exposure to cationic neurotoxins and bioactive amines.

The choroid plexus (CP) forms the blood-cerebrospinal fluid (CSF) barrier and protects the brain from circulating metabolites, drugs, and toxins. The plasma membrane monoamine transporter (PMAT, SLC29A4) is a new polyspecific organic cation transporter that transports a wide variety of organic cations including biogenic amines, cationic drugs, and neurotoxins. PMAT is known to be expressed in the CP, but its specific role in CP transport of organic cations has not been clearly defined. Here we showed that PMAT transcript is highly expressed in human and mouse CPs, whereas transcripts of other functionally related transporters are minimally expressed in the CPs. Immunofluorescence staining further revealed that PMAT protein is localized to the apical (CSF-facing) membrane of the CP epithelium, consistent with a role of transporting organic cations from the CSF into CP epithelial cells. To further evaluate the role of PMAT in the CP, mice with targeted deletion of the *Slc29a4* gene were generated and validated. Although *Pmat*$^{-/-}$ mice showed no overt abnormalities, the uptake of monoamines and the neurotoxin 1-methyl-4-phenylpyridinium was significantly reduced in CP tissues isolated from the knock-out mice. Together, our data demonstrated that PMAT is a major transporter for CP uptake of bioactive amines and xenobiotic cations. By removing its substrates from the CSF, PMAT may play an important role in protecting the brain from cationic neurotoxins and other potentially toxic organic cations.

The mammalian brain is protected from circulating metabolites, neuroactive substances, drugs, toxins, and blood-borne pathogens by two major permeability barriers: the blood-brain barrier and the blood-cerebrospinal fluid barrier (BCSFB).[2] BCSFB is anatomically defined by the choroid pl]eexus (CP) epithelium located in the four brain ventricles. Besides secreting CSF, CP epithelial cells express many solute carrier and ATP-binding cassette transporters to actively transport compounds into or out of the brain (1–3). However, compared with the blood-brain barrier, relatively little is known about CP transporters and their roles in brain disposition of endogenous as well as foreign substances. Recent studies using transporter gene KO animals have suggested that CP could play a significant role in influencing CSF concentrations and brain bioavailability and exposure to nutrients, drugs, and toxins (4–6). For example, the sodium-dependent vitamin C transporter 2 (Svct2, *Slc23a2*), which is absent from the blood-brain barrier but highly expressed in the CP at the basolateral (blood-facing) membrane, plays a major role in supplying the brain with ascorbic acid (7). The proton-coupled oligopeptide transporter 2 (Pept2, *Slc15a2*) expressed at the apical (CSF-facing) membrane mediates substrate uptake from the CSF (8). *Pept2* knock-out mice showed reduced CP uptake of dipeptides and peptidomimetic drugs and are more susceptible to 5-aminolevulinic acid-induced neurotoxicity (9, 10).

Many CNS active compounds, such as the endogenous monoamine neurotransmitters, trace amines, neurotoxins (*e.g.*, 1-methyl-4-phenylpyridinium (MPP^+)), and drugs, are organic cations (OCs) that rely on monoamine and organic cation transporters to cross membrane barriers. Earlier studies showed that the CP is able to accumulate monoamine neurotransmitters against a concentration gradient (11). Within the CP, biogenic amines are metabolized by monoamine oxidase and catechol-*O*-methyltransferase (11–13), suggesting CP acts as both a structural and an enzymatic barrier to regulate CNS homeostasis of endogenous amines. Moreover, CP expresses transport activities for xenobiotic OCs with diverse chemical structures (14, 15). This OC transport system may play an active role in clearing cationic drugs, drug metabolites, and neurotoxins from the brain (2, 16). However, little is pres-

* This work was supported, in whole or in part, by National Institutes of Health Grants GM066233 and GM066233-07S1 (to J. W.). This work was also supported by National Disease Research Interchange with support from National Institutes of Health Grant 5 U42 RR006042.

[1] To whom correspondence should be addressed: Dept. of Pharmaceutics, University of Washington, H272J Health Science Bldg., Seattle, WA 98195. Tel.: 206-221-6561; Fax: 206-543-3204; E-mail: jowang@uw.edu.

[2] The abbreviations used are: BCSFB, blood-cerebrospinal fluid barrier; PMAT, plasma membrane monoamine transporter; OC, organic cation; CP, choroid plexus; CSF, cerebrospinal fluid; D22, decynium-22 (1,1′-diethyl-2,2′-cyanine); MPP^+, 1-methyl-4-phenylpyridinium; DAT, dopamine transporter; NET, norepinephrine transporter; OCT, organic cation transporter; SERT, 5-HT transporter; MATE, multidrug and toxin extrusion; 5-HT, 5-hydroxytryptamine.

ently known regarding the molecular mechanisms underlying monoamine and OC transport in the CP. Although several transporters, including the serotonin transporter (SERT) and organic cation transporters 1–3 (OCT1–3), have been implicated in this process (2, 17, 18), the expression and membrane localization for most of these transporters have not been well analyzed in native CP tissues. Furthermore, there is essentially no functional data supporting a specific role of these transporters in CP uptake and transport of endogenous amines and xenobiotic OCs.

Plasma membrane monoamine transporter (PMAT, SLC29A4) is a new polyspecific OC transporter first cloned and characterized in our laboratory (19, 20). PMAT functions as a Na^+-independent, electrogenic, and polyspecific transporter that shares a large substrate and inhibitor overlap with OCT1–3 in the SLC22 family. Prototype PMAT substrates include biogenic amines, MPP^+ and MPP^+-like neurotoxins, and clinically used drugs (20–22). Abundantly expressed in multiple brain regions, PMAT represents a major uptake 2 transporter for serotonin (5-HT) and dopamine in the CNS (22). Previous work by Vialou *et al.* (23) and by us (24) showed that PMAT mRNA is highly expressed in mouse and rat CPs. Our expression profiling analysis of 252 *Slc* transporter genes in the Allen Brain Atlas further identified *Pmat* as one of a few *Slc* genes with the highest expression intensity in the CP (25). Okura *et al.* (26) also recently reported a dominating expression of *Pmat* mRNA over *Oct1–3* in an immortalized cell line derived from rat CP. Based on these data, we hypothesize that PMAT is a major component of the OC transport system at the BSCFB and plays an important role in CP transport of endogenous and xenobiotic OCs. In this study, we carried out detailed analysis to determine the role of PMAT at the BCSFB. We first analyzed the expression profile of known monoamine and organic cation transporters in rodent and human CP tissues. The membrane localization of PMAT is then determined by immunofluorescence microscopy. Finally, the functional significance of PMAT in OC transport at the BCSFB is demonstrated by developing and utilizing a mouse model with targeted deletion of the *Slc29a4* gene.

EXPERIMENTAL PROCEDURES

Materials—[^{3}H]MPP^+ (85 Ci/mmol) and [^{14}C]mannitol (50 mCi/mmol) were purchased from American Radiolabeled Chemicals, Inc. [^{3}H]5-HT (28 Ci/mmol) and [^{3}H]dopamine (51.3 Ci/mmol) were purchased from PerkinElmer Life Sciences. Nonradiolabeled chemicals were purchased from Sigma-Aldrich. Cell culture media and reagents were from Invitrogen. Cell culture plastic wares were from BD Biosciences or Corning.

Quantification of Transporter mRNA Expression by Real Time PCR—Mouse CPs were dissected from the lateral and fourth ventricles of brain after euthanization with CO_2. Total RNA was extracted from mouse CP or whole brain using TRIzol reagent (Invitrogen). Human CP epithelial cell total RNA was purchased from ScienCell Research Laboratories (Carlsbad, CA). After reverse transcription with Superscript III (Life Technologies, Inc.) into cDNA, the expression levels of selected transporter genes were quantified with TaqMan real time PCR as described previously (22). The validated primer and probe assay sets for assayed genes were purchased from Applied Biosystems, Inc. Their assay IDs are: Mm01250065_m1 (*Sert*), Mm00438396_m1 (*Dat*), Mm00436661_m1 (*Net*), Mm00488294_m1 (*Oct3*), Mm01197698_m1 (*Gusb*, β-glucuronidase), Mm00525578_m1 (*Pmat*), Mm00456308_m1 (*Oct1*), Mm00457295_m1 (*Oct2*), Mm00840361_m1 (*Mate1*), Mm02601002_m1 (*Mate2*), Hs01085703_g1 (*PMAT*), Hs00427554_m1 (*OCT1*), Hs00161893_m1 (*OCT2*), Hs00222691_m1 (*OCT3*), Hs00997364_m1 (*DAT*), Hs00984348_m1 (*SERT*), Hs01567442_m1 (*NET*), Hs00979028_m1 (*MATE1*), and Hs00945650_m1 (*MATE2*). All of the samples were run in triplicate. The relative expression level of each gene in the CP was normalized to a reference gene, *GAPDH*.

Western Blot and Immunofluorescence Staining of PMAT in Choroid Plexus—Human CP tissues were obtained from the National Disease Research Interchange (Philadelphia, PA). For Western blot, CP tissues were mixed with 1 ml of ice-cold homogenization buffer containing 10 mM Tris-HCl, pH 7.4, 250 mM sucrose, 10 mM KH_2PO_4, 5 mM EDTA, 1 mM phenylmethylsulfonyl fluoride, and protease inhibitor mixture (Roche Applied Science). After homogenization, tissue homogenates were centrifuged at 600 × *g* for 5 min at 4 °C. The supernatant was transferred to a new centrifuge tube and centrifuged at 10,000 × *g* for 15 min at 4 °C. The supernatant was then harvested. Protein concentrations were determined with a BCA protein assay kit (Bio-Rad). Protein samples (100 μg) were subjected to SDS-PAGE. The blot was incubated with a previously developed and validated anti-PMAT polyclonal antibody P469 (1:500) (24) and followed by detection with a horseradish peroxidase-conjugated goat anti-rabbit IgG (1:20,000 dilution).

For immunofluorescence staining, frozen sections of human CP tissues (4 μm in thickness) were fixed with ice-cold acetone for 10 min, dried, and rehydrated in phosphate-buffered saline. They were then blocked with a blocking buffer (10% FBS, 0.1% Triton X-100 in PBS) for 90 min and then incubated with the primary antibody diluted in blocking buffer (1:200) overnight at 4 °C. PMAT was detected with the P469 polyclonal antibody. Na^+/K^+-ATPase was detected with a monoclonal anti-Na^+/K^+-ATPase α subunit antibody (Sigma). The next day, CP sections were washed three times with a washing buffer (0.05% Tween 20, PBS) and then incubated with 1:5000 dilutions of Alexa Fluor 488-conjugated donkey anti-rabbit and Alexa Fluor 555-conjugated goat anti-mouse secondary antibodies (Invitrogen) for 1 h at room temperature. CP sections were then washed three times and then mounted with ProLong Gold antifade reagent (Molecular Probes, Eugene, OR). For localization in mouse CP, freshly isolated mouse CP tissues were fixed with 4% paraformaldehyde, washed with PBS, and quenched with 50 mM NH_4Cl in PBS. After washing with PBS, the CP tissues were permeabilized with 0.2% Triton X-100 in PBS for 30 min, blocked with a blocking buffer (10% FBS, 0.1% Triton X-100 in PBS), and then incubated with 1:200 dilution of the PMAT antibody P469 in blocking buffer overnight at 4 °C with shaking. The next day, CP tissues were washed three times with washing buffer (0.05% Tween 20, PBS) and then incubated with 1:10,000 Alexa Fluor 488-conjugated goat anti-rabbit secondary anti-

body (Invitrogen) for 1 h at room temperature. CP tissues were then washed three times, immersed in Fluoromount G solution (SouthernBiotech, Inc.), and mounted on a glass slide. Fluorescence signals were detected with a Zeiss 510 META confocal imaging system or a Zeiss Axiovert 200 fluorescence microscope.

Slc29a4 Gene Targeting and Generation of Pmat Null Mice—The mice used in the current study were housed in a centralized specific pathogen-free facility at the University of Washington. All of the procedures involving mice were approved by the Institutional Animal Care and Use Committee at the University of Washington. To construct the targeting vector, a 3.95-kb fragment within intron 2 and a 1.67-kb fragment spanning exons 8 and 9 of the murine *Slc29a4* gene were amplified by *Pfu*-Ultra high fidelity polymerase to use as long and short arms for the targeting vector (see Fig. 1). The two arms were designed to remove exons 3–7 of the *Slc29a4* gene upon homologous recombination. The long and short arms were cloned into the XbaI/KpnI and XhoI/NotI sites of the 4517D1 targeting vector kindly provided by Dr. Richard Palmiter at the University of Washington. The resulting 4517D1/Pmat targeting vector contains neomycin resistance gene for positive selection and PGK-DTA and HSV-TK cassettes for negative selection. The long and short arms were fully sequenced and aligned with mouse genomic DNA to confirm integrity. 50 μg of the linearized vector was then transfected into G4 ES cells (27) by electroporation and selected with neomycin and gancyclovir. Drug-resistant colonies were expanded and screened for homologous recombination by PCR. A total of 340 ES cell clones were screened, from which two homologous recombinants were identified. One clone was successfully expanded, and recombination was confirmed by Southern blot. The ES cell clone was then used for blastocyst injection into C57BL/6J embryos to generate chimeric mice. The chimeric males were crossed with C57BL/6J females, and germ line transmission was identified by PCR genotyping. The F0 $Pmat^{+/-}$ heterozygotes were then interbred to generate WT ($Pmat^{+/+}$) and KO ($Pmat^{-/-}$) offspring, which were identified by PCR genotyping and confirmed by Southern blot. The F0 transgenic mice were continuously backcrossed with wild-type C57BL/6J mice from Jackson Laboratory for more than seven generations to obtain genetically pure (>99% C57BL/6J background) Pmat KO mice. Pmat KO mice of generations F7–F9 were used for functional uptake studies. Base-line blood chemistry in WT and KO mice was determined using a commercial service at Phoenix Central Laboratory (Mukilteo, WA).

Southern Blot of Genomic DNA and PCR Genotyping—The Illuminator™ chemiluminescent detection system (Stratagene, Inc.) was used for nonradioactive Southern blot. Fluorescent probes were generated with the Prime-It® Fluor fluorescence labeling kit (Stratagene, Inc.) using a PCR fragment spanning exons 8 and 9 as the template. 10 μg of genomic DNA from ES cells or mouse tissues were digested with the enzyme StuI, separated on agarose gel, and transferred to nylon membrane by capillary action overnight. The membrane was hybridized with the fluorescent probe, washed according to manufacturer's instructions, and visualized by exposing to film.

For PCR genotyping, two sets of primers were designed to detect a region between exons 3 and 4 of the *Slc29a4* gene and the neomycin resistance gene, respectively. The primer sets are expected to generate PCR products of 847 bp for WT mice and 447 bp for KO mice in duplex PCRs using genomic DNA extracted from mouse ear clippings.

Functional Characterization of Truncated Pmat Transcript—*Pmat*-related transcripts expressed in $Pmat^{+/+}$ and $Pmat^{-/-}$ mice were amplified by RT-PCR with *Pfu*-Ultra polymerase from mouse brain. The forward primer lies 5′ of the ATG start codon in exon 2, and the reverse primer lies 3′ of the TGA stop codon in exon 11 of the wild-type *Slc29a4* gene, so transcripts generated from both the WT and the recombinant loci were amplified. The cDNAs were cloned into the NheI/XhoI sites of the pcDNA5/FRT vector and stably expressed in the Flp-in HEK293 cells as described previously (22). Uptake experiments using radiolabeled tracer substrates were conducted as described previously (22).

Ex Vivo Uptake Studies in Freshly Isolated CPs from $Pmat^{+/+}$ and $Pmat^{-/-}$ Mice—Uptake studies in freshly isolated CP tissues were performed using previously described procedures (28). Briefly, freshly isolated CPs from $Pmat^{+/+}$ and $Pmat^{-/-}$ mice were rinsed in ice-cold artificial CSF buffer (aCSF, containing 10 mM glucose, 103 mM NaCl, 4.7 mM KCl, 1.2 mM KH_2PO_4, 2.5 mM $CaCl_2$, 1.2 mM $MgSO_4$, 1 mM sodium pyruvate, 25 mM $NaHCO_3$, pH 7.4, saturated with 95% O_2 and 5% CO_2), then transferred to aCSF buffer at room temperature, and incubated for 5 min. Uptake was initiated by transferring CP tissues to aCSF buffer containing a radiolabeled substrate (^{3}H-labeled 5-HT, dopamine, and MPP^+ as tracer) with or without inhibitors. In addition, ^{14}C-labeled mannitol was included in the uptake solution as a non-membrane-permeable extracellular space marker. After 5 min of incubation, uptake was stopped by aspirating away the substrate solution and washing the CP tissues three times with ice-cold aCSF buffer. CP tissues were solubilized by incubating with 1 M NaOH for 2 h at 50 °C and then neutralized with 1 M HCl. [^{3}H] and [^{14}C] radioactivity in the lysate was determined with liquid scintillation counting. Protein concentration in the lysate was determined with a BCA protein assay kit (Thermo Scientific, Inc.). Specific 5-HT, dopamine, and MPP^+ uptake was determined by correcting ^{3}H-labeled substrate counts with [^{14}C]mannitol counts and then normalizing with protein content. The formula used to determine specific substrate uptake is: specific substrate uptake = [^{3}H] counts in lysate-[^{14}C] counts in lysate × [^{3}H] counts in substrate solution/[^{14}C] counts in substrate solution (28).

RESULTS

PMAT Is the Predominant Organic Cation/Monoamine Transporter Expressed in CP—Previous *in situ* hybridization work by us (24, 25) and Vialou *et al.* (23) indicated that PMAT is highly expressed in mouse and rat CP. To compare the relative abundance of *Pmat* with other OC and functionally related monoamine transporters in the CP, we quantified mRNA expression level of the polyspecific OC transporters (*Oct1–3* and *Mate1–2*) and Na^+-dependent, high affinity monoamine transporters (*Sert*, *Dat*, and *Net*) in isolated mouse CP tissues by quantitative real time PCR (Fig. 1*A*). The results showed that

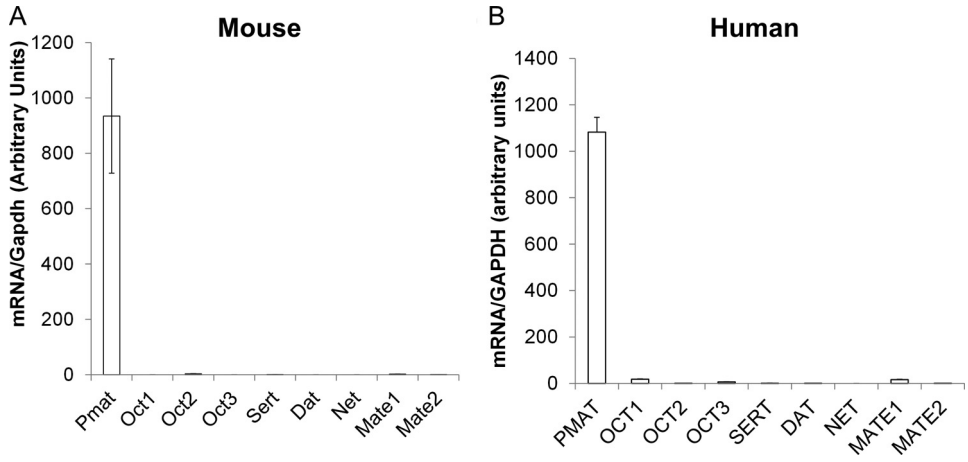

FIGURE 1. **Expression of *PMAT* and functionally related monoamine and OC transporters in choroid plexus.** Total RNA was extracted from WT mouse CPs (*A*) or human CP epithelial cells (*B*) and reverse transcribed. TaqMan quantitative real time PCR was used to determine the expression levels of the transporters. The *GAPDH* gene was used as an internal standard.

the *Pmat* transcript is expressed at much higher (300–10000-fold) levels than *Oct2*, *Sert*, *Mate1*, and *Mate2*. *Oct1*, *Oct3*, *Dat*, and *Net* were essentially not detectable in the mouse CP. These data demonstrated that *Pmat* is the predominant OC and monoamine transporter in the mouse CP. To determine whether this expression pattern is conserved in human CP, we further quantified the expression levels of human *PMAT*, *OCT1–3*, MATE1/2, *SERT*, *DAT*, and *NET* in purified human CP epithelial cells (Fig. 2*B*). The *PMAT* level was overwhelmingly higher (60–5000-fold) than *OCT1–3*, *SERT*, *DAT*, *MATE1*, and *MATE2*, whereas *NET* was undetectable (Fig. 2*B*). Together, these data clearly demonstrated that *PMAT* is the predominant OC and monoamine uptake transporter in both mouse and human CPs.

PMAT Protein Is Localized to the Apical Membrane of CP Epithelial Cells—The above data revealed a high and predominant expression of *PMAT* mRNA in the CP. We then analyzed PMAT protein expression in human CP using a PMAT-specific polyclonal antibody, P469, which was previously developed and validated in our laboratory (24, 29). Western blot analysis of human CP homogenate detected a strong band with expected molecular mass of human PMAT (58 kDa) (Fig. 2*A*). The localization of PMAT in human CP epithelial cells was examined through immunofluorescence staining of human CP sections with the PMAT polyclonal antibody P469. A monoclonal antibody against Na^+/K^+-ATPase, a specific apical membrane marker in CP epithelial cells (30, 31), was used as a control. As shown in Fig. 2*B*, PMAT labeling (*green*) was predominantly observed on the CSF-facing outer surface of the CP tissue and co-localized strongly with the Na^+/K^+-ATPase (*red*) as indicated by the *orange color* in the merged picture. These data clearly demonstrated that PMAT is localized to the CSF-facing apical membrane side of the CP epithelium, consistent with a role of transporting organic cations from the CSF into CP epithelial cells.

Generation of Mice with Targeted Deletion of Slc29a4 Gene—To elucidate the *in vivo* and tissue-specific roles of *Pmat* in OC and monoamine uptake, we aimed to generate a global knockout mouse model for *Pmat*. A targeting vector was constructed to replace exons 3–7 of the *Slc29a4* locus with the neomycin resistance gene (Fig. 3*A*). After homologous recombination, the recombinant locus was predicted to produce a transcript in which exon 2 of *Pmat* is spliced with exon 8 (Fig. 3*A*). Successful *Slc29a4* gene targeting in ES cells was identified by PCR amplification (data not shown). One recombinant clone was successfully expanded, and its homologous recombination status was further confirmed by StuI digestion and Southern blot analysis (Fig. 3*B*, *lane 2*). $Pmat^{+/-}$ F0 mice were interbred to generate F1 offspring with $Pmat^{+/+}$, $Pmat^{+/-}$, and $Pmat^{-/-}$ genotypes. The genotypes of these mice were identified by PCR amplification of genomic DNA extracted from ear clippings (Fig. 3*C*) and Southern blot (Fig. 3*B*, *lanes 3–5*).

Targeted Deletion of Slc29a4 Results in Defective mRNA Transcript Encoding a Nonfunctional Protein—The *Pmat* targeted allele, in which exon 2 is spliced with exon 8, was expected to result in multiple premature stop codons after the first 72 amino acids, generating a nonfunctional short peptide with only one partial transmembrane domain. To confirm the disruption of the Pmat function in the gene product, we amplified the full-length cDNA from mRNA isolated from $Pmat^{+/+}$ and $Pmat^{-/-}$ mouse brain (Fig. 4*A*) and cloned the cDNA products into pcDNA5 vector. The sequence of the cDNA cloned from the $Pmat^{-/-}$ mice completely aligned with the predicted sequence, whereas the cDNA from the $Pmat^{+/+}$ mice was identical to that previously reported for mouse Pmat (24). Both clones were then stably expressed in the Flp-in HEK293 cells, and uptake assays were performed. As shown in Fig. 4*B*, $Pmat^{+/+}$ cDNA transfected cells showed robust transport activities for MPP^+, 5-HT, and dopamine. In contrast, $Pmat^{-/-}$ cDNA transfected cells had no uptake activity for all of the tested substrates. These data demonstrated that the gene product from the *Slc29a4* locus in the $Pmat^{-/-}$ mice had no transport activity for OCs and monoamines.

No Compensatory Expression of Functionally Related Transporters in the Brain and CP in $Pmat^{-/-}$ Mice—$Pmat^{-/-}$ mice were viable, fertile with no overt physiological abnormalities. Blood chemistry determination showed no significant differences in base-line values of various serum biomarkers between WT and KO mice (Table 1). Quantitative real time PCR revealed that whole brain expression of functionally related

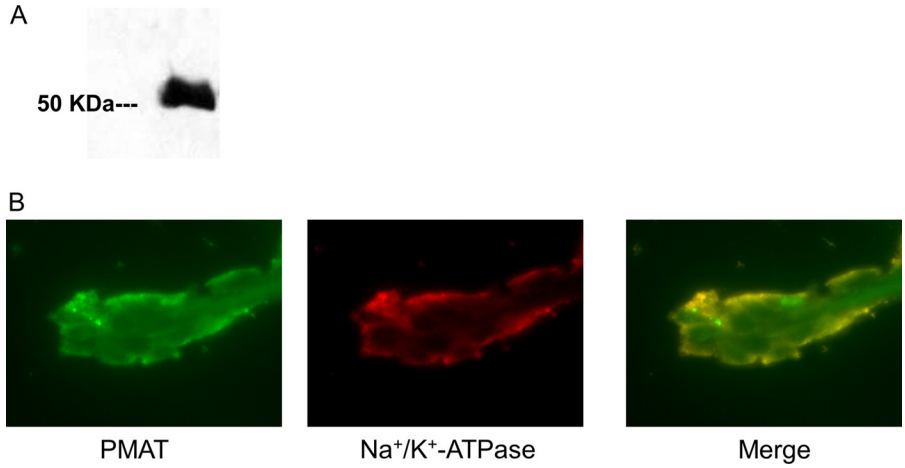

FIGURE 2. **Expression and localization of PMAT in human choroid plexus.** *A*, Western blot of human CP total protein using the PMAT polyclonal antibody P469. A strong band corresponding to PMAT molecular mass was detected. *B*, dual channel immunofluorescence staining of human CP frozen sections. PMAT (*green signal*) co-localizes with the CP apical membrane marker Na^+/K^+-ATPase (*red signal*).

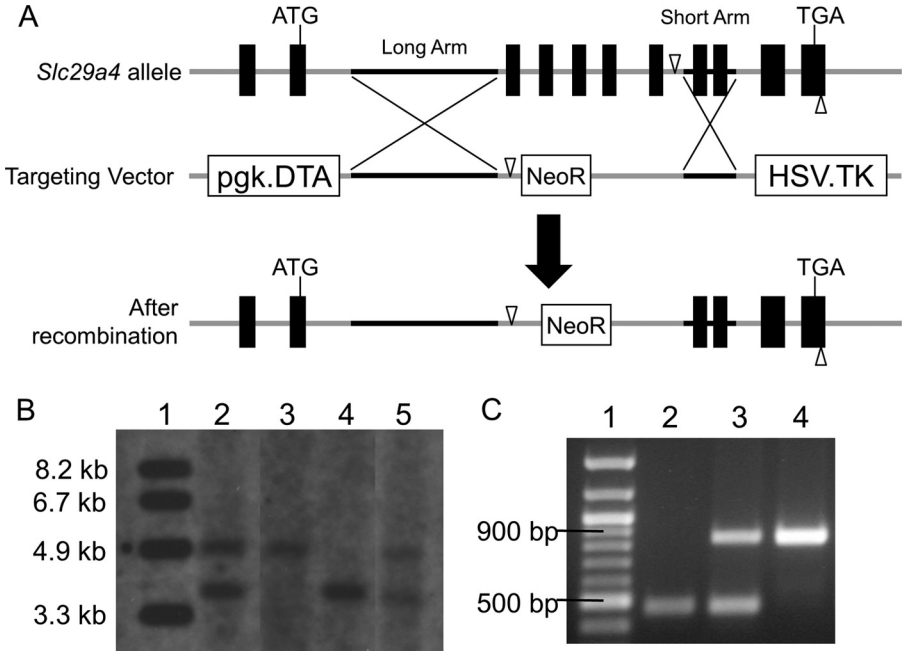

FIGURE 3. *A*, schematic diagram showing *Slc29a4* gene targeting strategy. The *black boxes* on the *Slc29a4* allele indicate exons. The start and stop codons are noted. The genomic regions cloned into long and short arms are indicated with *black lines*. The *open triangles* represent StuI digestion sites used for Southern blot. *B*, Southern blot of genomic DNA digested with StuI to confirm homologous recombination. *Lane 1*, molecular mass marker; *lane 2*, ES cell clone used for blastocyst injection; *lane 3*, $Pmat^{-/-}$ mouse; *lane 4*, $Pmat^{+/+}$ mouse; *lane 5*, $Pmat^{+/-}$ mouse. The expected band sizes are 3.5 kb for WT allele and 4.6 kb for *Pmat* null allele. *C*, PCR genotyping using genomic DNA from mice. *Lane 1*, molecular mass marker; *lane 2*, $Pmat^{-/-}$ mouse; 3, $Pmat^{+/-}$ mouse; *lane 4*, $Pmat^{+/+}$ mouse. The expected band sizes are 847 bp for WT allele and 447 bp for *Pmat* null allele.

transporters (*Sert*, *Dat*, *Net*, *Oct3*) were not changed by *Pmat* deletion (Fig. 5*A*). In the CP, no compensatory changes were detected in *Oct1–3*, *Sert*, *Dat*, *Net*, or *Mate1–2* (Fig. 5*B*).

Impaired OC and Monoamine Uptake in CP of $Pmat^{-/-}$ Mice—There was no observable difference in CP size and morphology between $Pmat^{+/+}$ and $Pmat^{-/-}$ mice. Immunofluorescence staining further confirmed an apical expression of Pmat protein in WT mouse CP. In contrast, no specific Pmat staining was observed in CP from KO mice (Fig. 6). To determine the functional significance of Pmat to CP uptake of OCs and monoamines, *ex vivo* uptake studies were performed with freshly isolated CP from WT and KO mice. CP tissues were incubated in uptake buffer containing a ^{3}H-labeled OC substrate (MPP^+, 5-HT, and dopamine) and [^{14}C]mannitol (to correct for extracellular space). Uptake activity was determined after correction for extracellular space and was normalized to protein content as described under "Experimental Procedures." As shown in Fig. 7*A*, for all three substrates tested, the overall uptake from the KO CP was ~30–40% lower than that in WT CP. Nonspecific uptake, as determined with saturating concentration (20 mM) of the unlabeled substrate, comprised ~10–20% of the total uptake and was similar between WT and KO CPs (Fig. 7*A*).

We then compared the uptake of MPP^+ in the presence of D22 and corticosterone. At the concentrations used, D22 (20 μM) inhibits both PMAT and OCT1–3, whereas corticosterone

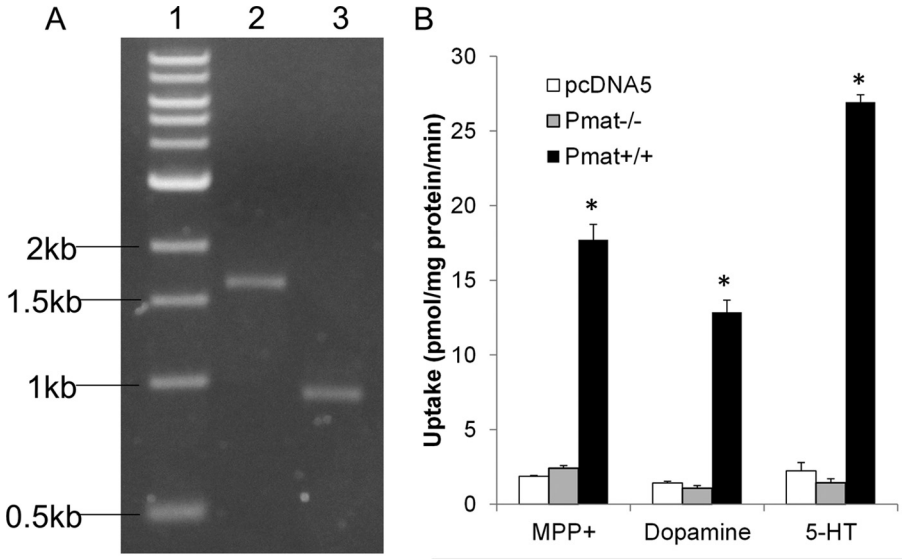

FIGURE 4. *A*, *Pmat* cDNA amplified from total RNA of WT and *Pmat*$^{-/-}$ mouse brain. *Lane 1*, molecular mass marker; *lane 2*, WT mouse; *lane 3*, *Pmat*$^{-/-}$ mouse. The expected cDNA sizes are 1627 bp for the WT allele and 932 bp for *Pmat* null allele. *B*, functional analysis of cells stably transfected with cDNA encoding the *Slc29a4* gene product either from WT or KO mice. cDNAs amplified in *A* were cloned into the pcDNA5/FRT expression vector and stably expressed in Flp-in HEK293 cells. Uptake studies were conducted with cells stably transfected with product amplified from WT or KO brain along with the pcDNA5 empty vector. The PMAT substrates MPP^+, dopamine, and 5-HT were used. The results represent the means ± S.D. of three independent experiments. *, $p < 0.05$ compared with pcDNA5 vector control.

TABLE 1

Base-line blood chemistry parameters of Pmat$^{+/+}$ and Pmat$^{-/-}$ mice (n = 3–10 for each genotype)

No statistical significance was detected between *Pmat*$^{+/+}$ and *Pmat*$^{-/-}$ mice ($p > 0.05$). K, thousand; M, million.

	Pmat$^{+/+}$	*Pmat*$^{-/-}$
Glucose (mg/dl)	143 ± 11	137 ± 8
Cholesterol (mg/dl)	97.4 ± 19.6	93.5 ± 18.0
Calcium (mg/dl)	11.21 ± 0.72	10.93 ± 0.23
Phosphorus (mg/dl)	9.53 ± 1.79	10.77 ± 0.32
Blood urea nitrogen (mg/dl)	26.67 ± 9.02	19.67 ± 2.08
Albumin (g/dl)	3.73 ± 0.25	3.70 ± 0.10
Globulin (g/dl)	2.20 ± 0.00	2.20 ± 0.10
Alkaline phosphatase (units/liter)	119.3 ± 49.5	117.7 ± 41.8
Alanine aminotransferase (units/liter)	37.0 ± 13.0	32.3 ± 6.7
White blood cell (K/μl)	4.27 ± 0.22	4.15 ± 1.56
Red blood cell (M/μl)	9.96 ± 0.79	10.08 ± 0.49
Hemoglobin (g/dl)	14.69 ± 1.11	14.57 ± 1.70
Thyroxine T4 (μg/dl)	3.67 ± 0.65	3.57 ± 1.33

(50 μM) inhibits OCT1–3 but not PMAT (32). As shown in Fig. 7*B*, D22 but not corticosterone inhibited MPP^+ uptake in CP from WT mice, whereas neither D22 nor corticosterone had an effect on MPP^+ uptake in KO CP. Furthermore, D22 reduced MPP^+ uptake in WT CP to the same level of MPP^+ uptake in KO CP, suggesting that the D22-sensitive component of OC uptake is attributable to Pmat. In contrast, Oct1–3, which are sensitive to inhibition by corticosterone (32), play an insignificant role in OC uptake in the CP.

No Significant Contribution of High Affinity Transporters to OC and Monoamine Uptake in the CP—We also examined the contribution of the high affinity monoamine transporters (SERT, DAT, and NET) to OC and monoamine uptake in mouse CP by using a pan inhibitor RTI-55 (33). *In vitro* uptake experiments using stably transfected Flp-in HEK293 cells confirmed that RTI-55 is a highly potent inhibitor for SERT, DAT, and NET ($IC_{50} < 30$ nM), but not for PMAT ($IC_{50} > 100$ μM; Table 2). As shown in Fig. 8, RTI-55 (1 μM) had no significant effect on the uptake of MPP^+, 5-HT, or dopamine in WT CP, indicating that the high affinity transporters do not significantly contribute to their uptake. RTI-55 also had no effect on OC and monoamine uptake in CP from KO mice (data not shown). We also checked whether monoamine oxidases may affect the uptake of monoamine substrates in CP. As shown in Fig. 8, pargyline (10 μM), a nonspecific monoamine oxidase inhibitor, had no effect on the uptake of MPP^+, 5-HT, or dopamine in WT CP, suggesting that under the conditions used in our CP uptake assay, monoamine metabolism does not confound uptake analysis.

DISCUSSION

The CP is a highly vascularized structure in the mammalian brain and acts as an anatomical and functional barrier between the CSF and the blood. CP epithelial cells are polarized with tightly sealed junctions. The basolateral membrane of the CP epithelium is perfused with blood, whereas the apical membrane is in free contact with the CSF. Like the blood-brain barrier, CP (or BCSFB) employs a wide array of membrane transporters to facilitate solute exchange between the CNS and the blood. In this study, we demonstrated that PMAT, a Na^+-independent, electrogenic transporter, is a major OC/monoamine transporter in the CP. Immunolocalization further revealed that PMAT protein is localized to the apical membrane of the CP epithelium, consistent with a role of transporting OC and monoamines from the CSF into CP epithelial cells. The functional significance of PMAT in CP uptake of OCs and monoamines was further demonstrated by generating and utilizing a knock-out mouse model of *Pmat*.

Earlier studies showed that CP is able to accumulate monoamine neurotransmitters and transports positively charged xenobiotics from CSF to blood (11). Using isolated CP and primary culture cells, Villalobos *et al.* (34) showed that OC uptake at the apical membrane is carrier-mediated. Although it is gen-

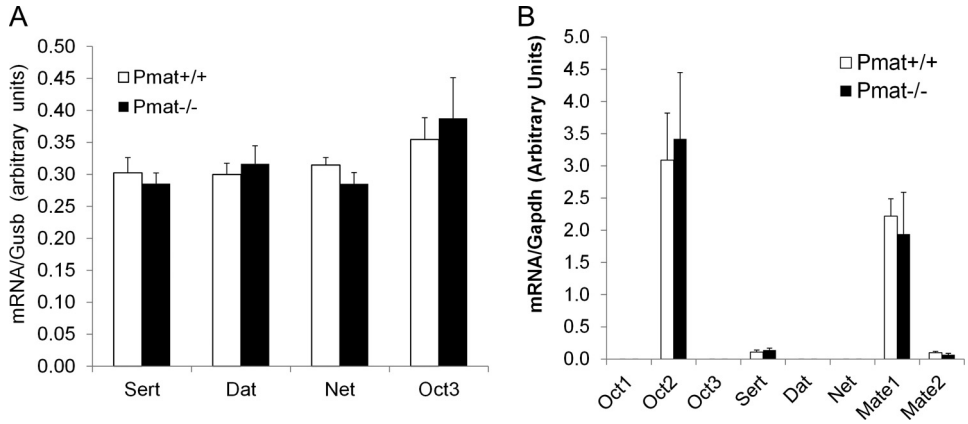

FIGURE 5. **No compensatory changes in the expression of functionally related monoamine and OC transporters in *Pmat*$^{-/-}$ mice.** Total RNA was extracted from whole brain (*A*) or CP tissues (*B*) of WT and *Pmat*$^{-/-}$ mice ($n = 4$ each genotype). Quantitative real time RT-PCR was used to determine the mRNA levels of the transporters. The data represent the means ± S.D. for four mice. No significant difference ($p > 0.05$) was found between WT and *Pmat*$^{-/-}$ mice for all transporters.

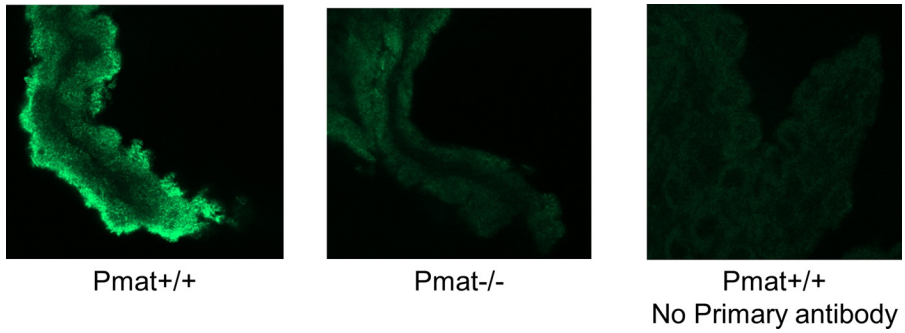

FIGURE 6. **Expression and localization of Pmat in mouse CP.** WT and *Pmat*$^{-/-}$ mouse CPs were isolated, fixed, permeabilized, and immunostained with the P469 anti-PMAT primary antibody and Alexa Fluor 488-conjugated secondary antibody. Confocal scanning sections of immunostained CP tissues are shown. The WT CP tissue without primary antibody incubation was used as a control.

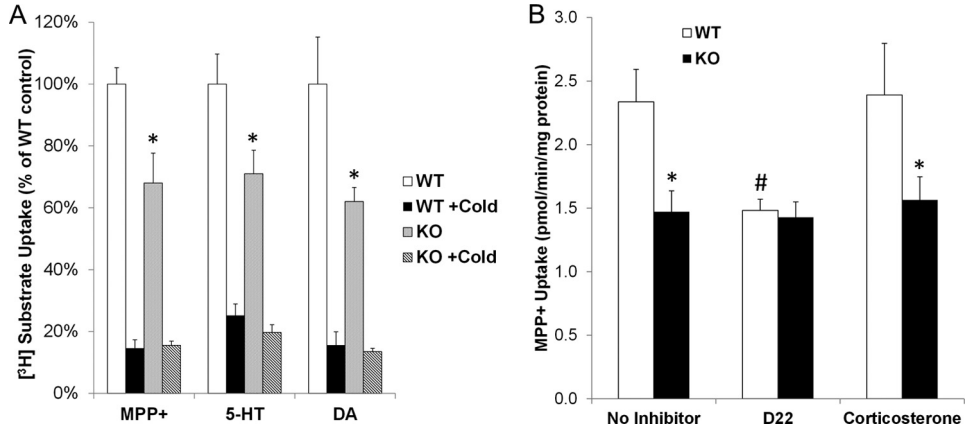

FIGURE 7. **Uptake of OC substrates in WT and *Pmat*$^{-/-}$ mouse CPs.** *Ex vivo* uptake in CPs isolated from WT and *Pmat*$^{-/-}$ mice was conducted as described under "Experimental Procedures." *A*, CP uptake rates were determined for the OC substrates MPP$^+$, 5-HT, and dopamine (*DA*) in the absence or presence of saturating concentrations (20 mM) of unlabeled substrates (indicated by *+Cold*). *B*, CP uptake rates were determined for MPP$^+$ with or without the inhibitors D22 (10 μM) and corticosterone (50 μM). The results represent the means ± S.D. of three independent experiments. *, $p < 0.05$ compared with WT CP; #, $p < 0.05$ compared with no inhibitor control.

erally believed that CP possesses a transport system to actively efflux OC from CSF to blood (2), the molecular identities of this transport system are poorly defined. Previously, OCT2 was suggested to be the transporter responsible for apical uptake of choline and other OCs (18). However, there is no direct evidence demonstrating the expression of OCT2 in the CP or its localization to the apical membrane. Gene profiling work by us and others showed very low expression of *Oct2* in rodent CPs (35). Here, using quantitative real time PCR, we clearly showed that in both human and mouse CP tissues, *PMAT/Pmat* is the dominating monoamine/OC transporter, whereas other functionally related transporters, including *OCT1*, *OCT2*, *OCT3*, *MATE1/2*, *SERT*, *DAT*, and *NET*, are minimally expressed (Fig. 1). The mRNA expression data are consistent with functional data showing no contribution of OCT1–3 to apical uptake of OCs in mouse CP (Fig. 7*B*).

TABLE 2

IC_{50} values of RTI-55 for human high affinity monoamine transporters and PMAT determined in stably transfected Flp-in HEK293 cells

The data represent the means ± S.D. of two or three independent experiments.

	IC_{50}
	*n*M
SERT	18.6 ± 2.2
DAT	29.6 ± 3.0
NET	23.2 ± 2.0
PMAT	>100,000

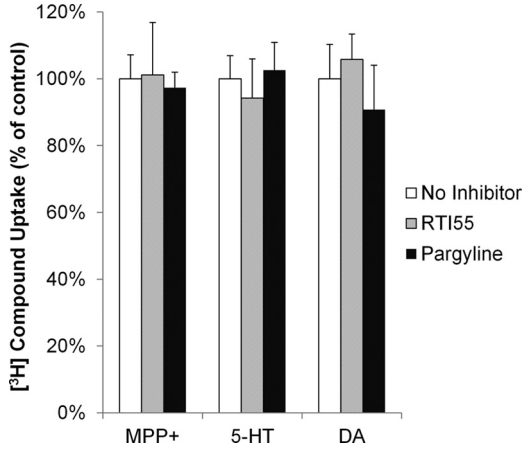

FIGURE 8. **Effects of the high affinity monoamine transporter inhibitor RTI-55 (1 μM) and the monoamine oxidase inhibitor pargyline (10 μM) on the uptake of MPP^+, 5-HT, and dopamine (*DA*) in WT mouse CP.** The potency and selectivity of the SERT, DAT, and NET inhibitor RTI-55 were validated in Table 2. The results represent the means ± S.D. of three independent experiments.

Consistent with the real time PCR data, the 58-kDa PMAT protein was easily detectable in human CP homogenate by Western blot (Fig. 2*A*). An immunolocalization study clearly revealed an apical membrane localization of PMAT in human and mouse CP epithelial cells (Figs. 2*B* and 6), which is consistent with its apical localization in other epithelial cells (36). The membrane localization of PMAT in CP cells corroborates a role of this transporter in the uptake of substrate from the CSF into CP epithelial cells, the first step of OC efflux at the BCSFB. Recent electrophysiological work from our laboratory unequivocally demonstrated that PMAT functions as an electrogenic transporter and that PMAT-mediated OC uptake is associated with inwardly directed currents that are strongly dependent on membrane potential and pH of the perfusate (37). Therefore, the physiological inside-negative membrane potential in CP epithelial cells would serve as a driving force for OC accumulation against a substrate concentration gradient. In addition, the activity of PMAT is known to be stimulated by an acidic extracellular pH. Although the pH of the bulk CSF is similar to that of plasma, a proton-rich microenvironment near the CP apical domain has been proposed to provide a driving force of proton-coupled transporters such as PEPT2 (38, 39). If such a microenvironment indeed exists, it could serve as an additional driving force to energize PMAT-mediated OC uptake into CP epithelial cells.

Once inside the CP epithelial cells, OCs and monoamines could be metabolized by intracellular enzymes or further effluxed into the blood at the basolateral membrane. Currently, little is known regarding the mechanisms underlying OC efflux at the basolateral membrane. Our real time PCR data showed that *MATE1/2*, the H^+/OC exchangers responsible for the final OC excretion step in renal and hepatic epithelial cells (40), are expressed at very low levels in mouse and human CPs and thus may not play a major role in OC efflux at the basolateral membrane. Interestingly, using a fluorescent OC probe, Miller *et al.* (15) provided evidence that basolateral efflux of OC compounds may occur through a vesicular transport mechanism independent of a carrier-mediated pathway.

To further confirm the role of PMAT in OC and monoamine transport in the CP, we generated mice with targeted deletion of the *Slc29a4* gene. Successful homologous recombination was confirmed by Southern blot and PCR (Fig. 3). Complete loss of transport activity was verified for the gene product generated from the targeted *Slc29a4* locus in KO mice (Fig. 4). The lack of an overt phenotype in $Pmat^{-/-}$ mice indicates that this transporter is physiologically nonessential under normal conditions. We did not detect any compensatory changes in the expression of functionally related monoamine/OC transporters in the brain and CP tissues in $Pmat^{-/-}$ mice (Fig. 5). Utilizing our *Pmat* knock-out mouse model, we investigated the contribution of PMAT to apical uptake of OC substrates in isolated intact CP tissues that preserve the *in vivo* anatomy of CP with apical membrane facing the outside. *Ex vivo* uptake studies using isolated CP tissues consistently showed a substantial (~30–40%) decrease in CP uptake for all tested OC and monoamine substrates in $Pmat^{-/-}$ mice (Fig. 7). Using selective and nonselective inhibitors for OCT1–3 and PMAT, we further showed that the D22-inhibitable component of MPP^+ uptake in WT CP appears to be attributable to PMAT. Oct1–3, in contrast, make little contribution to apical uptake of MPP^+ in CP. Using RTI-55, a potent inhibitor of SERT, DAT, and NET (Table 2), we also showed that the Na^+-dependent high affinity monoamine transporters also do not contribute to apical uptake of monoamines and OCs in the CP (Fig. 8). Together, these data clearly demonstrated a major role of PMAT in mediating OC and monoamine transport at the BCSFB.

An intriguing observation is that in KO mice, there is still substantial radioactivity associated with the CP tissue. Because intact CP tissue was used in uptake assays, the total amount of radioactivity measured represents not only substrate transported into CP epithelial cells but also compound bound to tissue or penetrated into deeper vascular layers. A large portion of the radioactivity remaining in $Pmat^{-/-}$ CP could be due to nonspecific binding or deeper penetration that cannot be easily washed off during the washing step. Moreover, the CP is known to express several 5-HT and dopamine receptors at high levels (41–43), and binding of radiolabeled 5-HT, dopamine, and MPP^+ (a dopamine analog) to these receptors could contribute substantially to the radioactivity associated with the $Pmat^{-/-}$ CP. In addition, although we have excluded OCT1–3, SERT, DAT, and NET in CP uptake of OCs and/or monoamines, it is possible that a yet to be identified transporter may contribute to additional CP uptake of OC compounds.

The choroid plexus plays an important role in maintaining CSF homeostasis and regulating the extracellular environment of the CNS. Efflux systems of the CP are critical for the removal of xenobiotics and metabolic wastes from CSF. As an uptake

transporter on the apical side, PMAT mediates the first step in the process of OC efflux from the CSF to the blood. OC compounds cleared by PMAT from the CSF may include released endogenous monoamine neurotransmitters, cationic drugs, and toxins. By removing its substrates from the CSF, PMAT could play an important role in protecting the brain from cationic neurotoxins and other potentially toxic organic cations. In this context, it is noteworthy to point out that we recently reported that several β-carbolines (*e.g.*, harmalan and norharmanium) are transportable substrates of PMAT (44). β-Carbolines are naturally found analogs of MPP^+, a synthetic neurotoxin that produces Parkinson's syndrome in humans and animal models. CNS exposure to β-carbolines has been implicated as an environmental risk factor for Parkinson's disease (45, 46). The current study suggests that PMAT may play a role in removing MPP^+-like neurotoxins from the brain and thus may lower disease risks. Further investigation of this hypothesis will have important toxicological and clinical implications.

Acknowledgments—We thank Dr. Richard D. Palmiter for providing the 4517D1 targeting vector and Dr. Li Xia for assistance in Western blot. We also thank the Transgenic Resources Program at the University of Washington for the generation of the Pmat knock-out mice and Dr. Edward J. Kelly for many helpful comments on the transgenic work.

REFERENCES

1. Graff, C. L., and Pollack, G. M. (2004) Drug transport at the blood-brain barrier and the choroid plexus. *Curr. Drug Metab.* **5,** 95–108
2. Kusuhara, H., and Sugiyama, Y. (2004) Efflux transport systems for organic anions and cations at the blood-CSF barrier. *Adv. Drug Deliv. Rev.* **56,** 1741–1763
3. Redzic, Z. (2011) Molecular biology of the blood-brain and the blood-cerebrospinal fluid barriers. Similarities and differences. *Fluids Barriers CNS* **8,** 3
4. Hu, Y., Shen, H., Keep, R. F., and Smith, D. E. (2007) Peptide transporter 2 (PEPT2) expression in brain protects against 5-aminolevulinic acid neurotoxicity. *J. Neurochem.* **103,** 2058–2065
5. Leggas, M., Adachi, M., Scheffer, G. L., Sun, D., Wielinga, P., Du, G., Mercer, K. E., Zhuang, Y., Panetta, J. C., Johnston, B., Scheper, R. J., Stewart, C. F., and Schuetz, J. D. (2004) Mrp4 confers resistance to topotecan and protects the brain from chemotherapy. *Mol. Cell. Biol.* **24,** 7612–7621
6. Sweet, D. H., Miller, D. S., Pritchard, J. B., Fujiwara, Y., Beier, D. R., and Nigam, S. K. (2002) Impaired organic anion transport in kidney and choroid plexus of organic anion transporter 3 (Oat3 (Slc22a8)) knockout mice. *J. Biol. Chem.* **277,** 26934–26943
7. Sotiriou, S., Gispert, S., Cheng, J., Wang, Y., Chen, A., Hoogstraten-Miller, S., Miller, G. F., Kwon, O., Levine, M., Guttentag, S. H., and Nussbaum, R. L. (2002) Ascorbic-acid transporter Slc23a1 is essential for vitamin C transport into the brain and for perinatal survival. *Nat. Med.* **8,** 514–517
8. Shu, C., Shen, H., Teuscher, N. S., Lorenzi, P. J., Keep, R. F., and Smith, D. E. (2002) Role of PEPT2 in peptide/mimetic trafficking at the blood-cerebrospinal fluid barrier. Studies in rat choroid plexus epithelial cells in primary culture. *J. Pharmacol. Exp. Ther.* **301,** 820–829
9. Shen, H., Smith, D. E., Keep, R. F., Xiang, J., and Brosius, F. C., 3rd (2003) Targeted disruption of the PEPT2 gene markedly reduces dipeptide uptake in choroid plexus. *J. Biol. Chem.* **278,** 4786–4791
10. Smith, D. E., Hu, Y., Shen, H., Nagaraja, T. N., Fenstermacher, J. D., and Keep, R. F. (2011) Distribution of glycylsarcosine and cefadroxil among cerebrospinal fluid, choroid plexus, and brain parenchyma after intracerebroventricular injection is markedly different between wild-type and Pept2 null mice. *J. Cereb. Blood Flow Metab.* **31,** 250–261
11. Lindvall, M., Hardebo, J. E., and Owman, C. (1980) Barrier mechanisms for neutrotransmitter monoamines in the choroid plexus. *Acta Physiol. Scand.* **108,** 215–221
12. Kaplan, G. P., Hartman, B. K., and Creveling, C. R. (1981) Localization of catechol-*O*-methyltransferase in the leptomeninges, choroid plexus and ciliary epithelium. Implications for the separation of central and peripheral catechols. *Brain Res.* **204,** 353–360
13. Vitalis, T., Fouquet, C., Alvarez, C., Seif, I., Price, D., Gaspar, P., and Cases, O. (2002) Developmental expression of monoamine oxidases A and B in the central and peripheral nervous systems of the mouse. *J. Comp. Neurol.* **442,** 331–347
14. Suzuki, H., Sawada, Y., Sugiyama, Y., Iga, T., and Hanano, M. (1986) Transport of cimetidine by the rat choroid plexus in vitro. *J. Pharmacol. Exp. Ther.* **239,** 927–935
15. Miller, D. S., Villalobos, A. R., and Pritchard, J. B. (1999) Organic cation transport in rat choroid plexus cells studied by fluorescence microscopy. *Am. J. Physiol.* **276,** C955–C968
16. Spector, R. (2010) Nature and consequences of mammalian brain and CSF efflux transporters. Four decades of progress. *J. Neurochem.* **112,** 13–23
17. Pavone, L. M., Tafuri, S., Mastellone, V., Morte, R. D., Lombardi, P., Avallone, L., Maharajan, V., Staiano, N., and Scala, G. (2007) Expression of the serotonin transporter (SERT) in the choroid plexuses from buffalo brain. *Anat. Rec.* (*Hoboken*) **290,** 1492–1499
18. Sweet, D. H., Miller, D. S., and Pritchard, J. B. (2001) Ventricular choline transport. A role for organic cation transporter 2 expressed in choroid plexus. *J. Biol. Chem.* **276,** 41611–41619
19. Engel, K., Zhou, M., and Wang, J. (2004) Identification and characterization of a novel monoamine transporter in the human brain. *J. Biol. Chem.* **279,** 50042–50049
20. Engel, K., and Wang, J. (2005) Interaction of organic cations with a newly identified plasma membrane monoamine transporter. *Mol. Pharmacol.* **68,** 1397–1407
21. Zhou, M., Duan, H., Engel, K., Xia, L., and Wang, J. (2010) Adenosine transport by plasma membrane monoamine transporter. Reinvestigation and comparison with organic cations. *Drug Metab. Dispos.* **38,** 1798–1805
22. Duan, H., and Wang, J. (2010) Selective transport of monoamine neurotransmitters by human plasma membrane monoamine transporter and organic cation transporter 3. *J. Pharmacol. Exp. Ther.* **335,** 743–753
23. Vialou, V., Balasse, L., Dumas, S., Giros, B., and Gautron, S. (2007) Neurochemical characterization of pathways expressing plasma membrane monoamine transporter in the rat brain. *Neuroscience* **144,** 616–622
24. Dahlin, A., Xia, L., Kong, W., Hevner, R., and Wang, J. (2007) Expression and immunolocalization of the plasma membrane monoamine transporter in the brain. *Neuroscience* **146,** 1193–1211
25. Dahlin, A., Royall, J., Hohmann, J. G., and Wang, J. (2009) Expression profiling of the solute carrier gene family in the mouse brain. *J. Pharmacol. Exp. Ther.* **329,** 558–570
26. Okura, T., Kato, S., Takano, Y., Sato, T., Yamashita, A., Morimoto, R., Ohtsuki, S., Terasaki, T., and Deguchi, Y. (2011) Functional characterization of rat plasma membrane monoamine transporter in the blood-brain and blood-cerebrospinal fluid barriers. *J. Pharm. Sci.* **100,** 3924–3938
27. George, S. H., Gertsenstein, M., Vintersten, K., Korets-Smith, E., Murphy, J., Stevens, M. E., Haigh, J. J., and Nagy, A. (2007) Developmental and adult phenotyping directly from mutant embryonic stem cells. *Proc. Natl. Acad. Sci. U.S.A.* **104,** 4455–4460
28. Teuscher, N. S., Novotny, A., Keep, R. F., and Smith, D. E. (2000) Functional evidence for presence of PEPT2 in rat choroid plexus. Studies with glycylsarcosine. *J. Pharmacol. Exp. Ther.* **294,** 494–499
29. Xia, L., Zhou, M., Kalhorn, T. F., Ho, H. T., and Wang, J. (2009) Podocyte-specific expression of organic cation transporter PMAT. Implication in puromycin aminonucleoside nephrotoxicity. *Am. J. Physiol. Renal. Physiol.* **296,** F1307–F1313
30. Praetorius, J., and Nielsen, S. (2006) Distribution of sodium transporters and aquaporin-1 in the human choroid plexus. *Am. J. Physiol. Cell Physiol.* **291,** C59–C67
31. Kimura, T., Allen, P. B., Nairn, A. C., and Caplan, M. J. (2007) Arrestins and spinophilin competitively regulate Na+,K+-ATPase trafficking through association with a large cytoplasmic loop of the Na^+,K^+-ATPase. *Mol. Biol. Cell* **18,** 4508–4518

32. Koepsell, H., Lips, K., and Volk, C. (2007) Polyspecific organic cation transporters. Structure, function, physiological roles, and biopharmaceutical implications. *Pharm. Res.* **24,** 1227–1251
33. Torres, G. E., Gainetdinov, R. R., and Caron, M. G. (2003) Plasma membrane monoamine transporters. Structure, regulation and function. *Nat. Rev. Neurosci.* **4,** 13–25
34. Villalobos, A. R., Parmelee, J. T., and Pritchard, J. B. (1997) Functional characterization of choroid plexus epithelial cells in primary culture. *J. Pharmacol. Exp. Ther.* **282,** 1109–1116
35. Choudhuri, S., Cherrington, N. J., Li, N., and Klaassen, C. D. (2003) Constitutive expression of various xenobiotic and endobiotic transporter mRNAs in the choroid plexus of rats. *Drug Metab. Dispos.* **31,** 1337–1345
36. Xia, L., Engel, K., Zhou, M., and Wang, J. (2007) Membrane localization and pH-dependent transport of a newly cloned organic cation transporter (PMAT) in kidney cells. *Am. J. Physiol. Renal. Physiol.* **292,** F682–F690
37. Itagaki, S., Ganapathy, V., Ho, H. T., Zhou, M., Babu, E., and Wang, J. (2012) Electrophysiological characterization of the polyspecific organic cation transporter plasma membrane monoamine transporter. *Drug Metab. Dispos.* **40,** 1138–1143
38. Smith, D. E., Johanson, C. E., and Keep, R. F. (2004) Peptide and peptide analog transport systems at the blood-CSF barrier. *Adv. Drug Deliv. Rev.* **56,** 1765–1791
39. Ho, H. T., Dahlin, A., and Wang, J. (2012) Expression profiling of solute carrier gene families at the blood-CSF barrier. *Front. Pharmacol.* **3,** 154
40. Otsuka, M., Matsumoto, T., Morimoto, R., Arioka, S., Omote, H., and Moriyama, Y. (2005) A human transporter protein that mediates the final excretion step for toxic organic cations. *Proc. Natl. Acad. Sci. U.S.A.* **102,** 17923–17928
41. Pasqualetti, M., Ori, M., Castagna, M., Marazziti, D., Cassano, G. B., and Nardi, I. (1999) Distribution and cellular localization of the serotonin type 2C receptor messenger RNA in human brain. *Neuroscience* **92,** 601–611
42. Roberts, J. C., Reavill, C., East, S. Z., Harrison, P. J., Patel, S., Routledge, C., and Leslie, R. A. (2002) The distribution of 5-HT(6) receptors in rat brain. An autoradiographic binding study using the radiolabelled 5-HT(6) receptor antagonist [^{125}I]SB-258585. *Brain Res.* **934,** 49–57
43. Mignini, F., Bronzetti, E., Felici, L., Ricci, A., Sabbatini, M., Tayebati, S. K., and Amenta, F. (2000) Dopamine receptor immunohistochemistry in the rat choroid plexus. *J. Auton. Pharmacol.* **20,** 325–332
44. Ho, H. T., Pan, Y., Cui, Z., Duan, H., Swaan, P. W., and Wang, J. (2011) Molecular analysis and structure-activity relationship modeling of the substrate/inhibitor interaction site of plasma membrane monoamine transporter. *J. Pharmacol. Exp. Ther.* **339,** 376–385
45. Collins, M., and Neafsey, E. (2000) β-Carboline analogues of MPP^+ as environmental neurotoxins, in *Neurotoxic Factors in Parkinson's Disease and Related Disorders* (Storch, A., and Collins, M. A., eds) pp. 115–130, Kluwer Academic Publishing/Plenum, New York
46. Nagatsu, T. (1997) Isoquinoline neurotoxins in the brain and Parkinson's disease. *Neurosci. Res.* **29,** 99–111